

J. M. Kendall, M. N. James,† and J. F. Knott**

The Behaviour of Physically Short Fatigue Cracks in Steels

REFERENCE Kendall, J. M., James, M. N., and Knott, J. F., **The Behaviour of Physically Short Fatigue Cracks in Steels**, *The Behaviour of Short Fatigue Cracks*, EGF Pub. 1 (Edited by K. J. Miller and E. R. de los Rios) 1986, Mechanical Engineering Publications, London, pp. 241-258.

ABSTRACT The behaviour of engineering or physically short fatigue cracks in two structural steels has been examined, using both through-thickness and thumbnail short crack geometries. The results indicate that much of the 'anomalous behaviour' of physically short cracks may be due to differences in the amount of closure experienced by long and short cracks. The prediction of fatigue life using a fracture mechanics approach is discussed and it is concluded that conservative life predictions may be based on a closure-free value of the threshold stress intensity range.

Introduction

The application of fracture mechanics to fatigue is based upon the assumption that the fatigue crack growth rate, da/dN , is a function of stress intensity range, $\Delta K = K_{\max} - K_{\min}$, and mean stress, often expressed as the load ratio, $R = K_{\min}/K_{\max}$. This approach provides a powerful method of calculating fatigue lives by integration of the da/dN versus ΔK relationship. For the integration to be performed, it is essential that the relationship holds for the whole range of crack lengths spanned by the limits of integration, which are usually taken as the initial defect size and the final crack length to cause failure. In these terms, the most general definition of the 'short crack problem' in fatigue is the situation when the functional relationships established between da/dN , ΔK , and R for long cracks do not hold.

Particular interest has been shown in the low growth rate or near-threshold region in which anomalies appear to be most in evidence. In this region the linear relationship between $\log da/dN$ and $\log \Delta K$, which is observed at higher growth rates, is no longer applicable, and the value of da/dN at successively lower values of ΔK tends asymptotically to the threshold stress intensity range, ΔK_{th} , below which long crack growth does not occur. It is still possible to calculate fatigue lives in the near-threshold region by integration if the da/dN versus ΔK long crack curve is fitted by a number of straight lines and each line is integrated separately (1). The behaviour of short cracks in the near-threshold

* Department of Metallurgy and Materials Science, University of Cambridge, Pembroke Street, Cambridge CB2 3QZ.

† Now at Department of Metallurgy and Materials Engineering, University of the Witwatersrand, 1 Jan Smuts Avenue, Johannesburg 2001, South Africa.

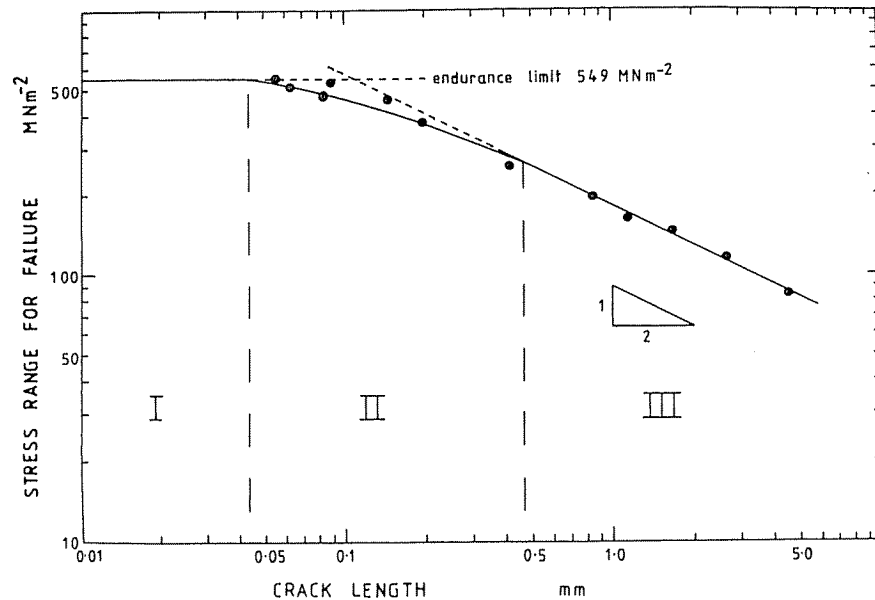


Fig 1 The 'Kitagawa plot' of applied stress range to cause failure against crack length, showing data of Kitagawa and Takahashi (8)

region is of importance because it has been observed in a large number of studies (see, for example, (1)–(7)) that fatigue crack growth can occur at elastically calculated values of ΔK that are lower than the long crack threshold ΔK_{th} .

The object of this paper is to explore the significance of physically short cracks in steels, with respect to engineering applications and the determination of the fatigue lives of structures and components. The experimental work presented has been carried out using two structural steels and it is of interest first of all to set the 'short crack problem' in the context of the engineering applications of these materials. Two general types of application which illustrate the S–N approach and the LEFM approach to fatigue design will be considered: machine components and engineering structures. One of the most convenient representations of short crack data is the 'Kitagawa plot' of applied stress range to cause failure, $\Delta\sigma_o$, against crack length, a , using logarithmic scales (8), as shown in Fig. 1. This shows clearly the regions of behaviour described by the S–N approach and the long crack LEFM approach to fatigue.

Machine components

In general, the moving components of machines are required to withstand a large number of fatigue cycles at relatively low applied stresses. For instance, an automobile engine that has travelled 100 000 miles at an average speed of 60

miles per hour and at 4000 revolutions per minute will have experienced 4×10^8 cycles. The fatigue design procedure is conventionally based on the endurance limit of the S–N curve, with appropriate correction factors for regions of stress concentration. Account may also be taken of the effect of surface hardening treatments on fatigue lifetimes.

The S–N curve is influenced by the size and distribution of defects in the material. A cast or wrought component typically contains an evenly distributed multiplicity of small defects of 1–100 μm in size. This is well below the limits of non-destructive testing (NDT) techniques, but a measure of defect control ('process control') can be achieved by controlling the size of defects produced during processing routes such as casting or hot working. Material containing a consistent population of small defects determined by process control fails when $\Delta\sigma_o$ exceeds the endurance limit (region T in Fig. 1).

In these applications fracture mechanics at present is conceptual and not quantitative, and the fatigue life of the component is determined directly from the S–N data. The 'short crack problem', in terms of design, is to determine whether the S–N curve for 'process-controlled' material can be non-conservative. There is, of course, scientific interest in examining the extent to which fracture mechanics can be extended to multiplicities of extremely small defects and situations in which components are designed to operate at applied stress ranges that exceed the endurance limit, when the number of cycles to failure may be less than 10^6 cycles (9)(10). The behaviour of 'microstructurally' short cracks originating at these small defects does not then follow the behaviour illustrated in region I in Fig. 1. The present paper, however, is concerned with 'physically' short cracks which are significantly larger than the microstructural unit, as considered in the following section.

Engineering structures

Many steel structures are fabricated by welding processes or by the use of rivets, and it is frequently found that defects of 0.1–2 mm in size are located in the region of these joints. Since static design stresses are typically of the order of two thirds of the yield stress, it should be possible to calculate the fatigue life by integration using a fracture mechanics approach. The loading spectrum in service will include a spread of applied stress ranges. If ΔK_{th} is appropriate, the integration can be carried out only for those stress ranges that produce ΔK values exceeding ΔK_{th} .

It can be seen from Fig. 1 that material initially containing a long crack would fail when ΔK exceeds the threshold ΔK_{th} (region III). The 'anomalous' behaviour of cracks which are physically short but several times larger than the microstructural unit is represented by region II. The significance of the position of the experimental data in this region is that both the S–N prediction and the LEFM prediction of $\Delta\sigma_o$ are non-conservative.

For long cracks, ΔK_{th} can be measured experimentally and related to the applied stress range at threshold. For short through-thickness cracks the value of ΔK is given by

$$\Delta K = Y \Delta \sigma (\pi a)^{1/2} \quad (1)$$

where Y is a constant for a given testpiece geometry, e.g. $Y = 1.12$ for an edge crack in a semi-infinite body. For short thumbnail cracks the value of ΔK is given by

$$\Delta K = Q \Delta \sigma (\pi a)^{1/2} \quad (2)$$

where Q refers to the ellipticity of the thumbnail crack. Therefore, by taking logarithms an expression of the following general form can be obtained

$$\log \Delta \sigma_o = \log \Delta K_{th} - \frac{1}{2} \log a + \text{constant} \quad (3)$$

In a number of critical applications, fatigue design and integrity in service are dependent on the sensitivity and reliability of the NDT technique that is employed, and on the ability of periodic NDT inspections to reveal fatigue crack growth. A general estimate of the limit of NDT for the majority of engineering structures is detection of a defect of 1–2 mm in size. Defects larger than the NDT limit can be eliminated by 'NDT control', but it must be assumed that defects up to that size exist in the structure, such as pre-existing weld defects which are physically small but large with respect to the microstructure generally.

It should be noted that the positions of the lines in Fig. 1 are altered by the magnitude of the mean tensile stress superimposed on the stress range applied during the fatigue cycle. It has long been recognized that the endurance limit is reduced by increasing the mean stress. Similarly, a reduction in the measured value of ΔK_{th} for long cracks is observed as the mean stress (i.e., load ratio, R) is increased. At high R values ($R > \text{approximately } 0.6$) there is minimal effect of closure on the near-threshold crack growth rate. An 'intrinsic material threshold', ΔK_c , may be defined as the measured ΔK_{th} at high load ratio, which is equal to the effective stress intensity range at threshold for all load ratios. From equation (3) it can be seen that a reduction in ΔK_{th} would lower the long crack LEFM line in Fig. 1 by reducing the $\log \Delta K_{th}$ term on the right hand side of the equation. This discussion will be developed later.

Types of short crack

Short cracks in steel structures and components are not uniform in their morphology, origin or stress state, and these factors may influence subsequent growth in fatigue. The common features from which short fatigue cracks may grow in steels can be broadly divided as follows.

(a) *Casting and weld defects.* Cast components frequently contain shrinkage

cavities that are formed on solidification and which may be associated with second phase particles. Weld defects such as lack-of-fusion defects are also formed on solidification of the weld metal. The residual stress fields associated with such defects may range from virtually zero (for a large, slowly-cooled casting in which sufficient diffusion can occur during cooling to relieve stresses induced by thermal contraction or phase changes) to yield point magnitude (for a rapidly-cooled weld in which negligible stress relief occurs during cooling). Studies of fatigue crack growth from natural casting defects in nickel–aluminium bronze (1) revealed no effect on propagation rate which could be attributed to residual stresses.

(b) *Hydrogen cracks.* Hydrogen cracks may form as a result of hydrogen embrittlement of steels and they may be associated with welds where 'hard spots' develop (11). The arrest of such cracks is associated with relieving plastic flow at the crack tips. The residual plasticity associated with short hydrogen cracks in iron – 3 per cent silicon single crystals has been revealed by etching (12) and found to be concentrated at the ends of the crack. However, the residual stresses are likely to be removed completely by a stress-relief heat treatment, e.g., a few hours at temperatures above 600°C.

(c) *Inclusions.* Second phase particles, including sulphides, oxides, intermetallic compounds and slag particles, frequently act as sites for fatigue crack initiation. During steel production the differing coefficients of thermal expansion in the inclusion and matrix give rise to differential strains at the interface between them. On cooling, these strains will result in residual tessellated stresses around the inclusions, which may be tensile or compressive (9)(13).

(d) *Quench cracks and surface damage.* A variety of surface hardening treatments may be applied to steel structures and components to extend their fatigue lives. Thermal, chemico-thermal, or mechanical treatments may be employed to provide both surface hardening and favourable compressive residual stresses. However, although the processes are designed to improve fatigue properties, they may be accompanied by the production of defects such as quench cracks or roughened surface profiles. Fatigue cracks originating from these sites will experience the effect of the residual stress fields resulting from the hardening treatment employed (14). Surface damage in the form of machining marks may also be produced by processes such as turning or grinding, where the depth of cut controls not only the size of a defect, but also the local stress field associated with it.

It is clear that the characteristics of the site at which a fatigue crack initiates can influence its early growth. Before any attempt is made to apply experimentally determined short crack data to engineering situations the types of short cracks involved must be taken into account. The methods of production of short

cracks for experimental work are generally concerned with two main geometries: through-thickness cracks and thumbnail (semi-elliptical) cracks.

Short through-thickness cracks may be prepared by growing a long crack and machining away the top surface to leave a crack that is short in the depth dimension (15)–(19): short thumbnail cracks may be initiated at small surface notches (8) or produced by growing a crack from a ridge that is subsequently removed by machining (20)(21). However, the most common method of obtaining short surface cracks that are approximately semi-elliptical in shape is by initiation at inclusions using smooth bar or hour-glass testpieces (1)–(6)(22). These testpieces may be subjected to stresses that exceed the yield stress at the surface, and so the short pre-crack grows under conditions of bulk plasticity. Even when the macroscopic applied stress is below the yield stress, the individual grains within which fatigue cracks initiate are locally yielded, and their early growth takes place within the local plastic field (4).

After preparation of short pre-cracks by these methods a stress-relief heat treatment may be applied to anneal out the plastically deformed material around the cracks. The aim is to leave a short pre-crack that is simply a geometric discontinuity. However, the effectiveness of common stress-relief treatments in achieving this is not certain, and a residual stress field may still exist around the short crack, particularly if the applied stresses have been high.

To summarize, if a fracture mechanics approach is to be used to describe the behaviour of physically short cracks in fatigue, it is essential to consider both the geometry of the cracks and the residual stress fields around them, whether produced during fabrication, surface-hardening, or testpiece preparation. The aim of the present paper is to attempt to do this using two well-characterized structural steels to examine the extent of the short crack problem in engineering structures. The work on the low strength steel is presented first.

Experimental work on a low strength steel

The material was a low carbon steel with a yield strength of 280 MNm^{-2} and an ultimate tensile strength of 420 MNm^{-2} , similar to the weldable structural steels used for the construction of railway bridges and railway vehicle bogies. The composition is shown in Table 1. The cast ingot was rolled and forged to $20 \times 40 \text{ mm}$ cross-section bars from which the testpieces were machined. The material had a ferrite-pearlite microstructure, as shown in Fig. 2(a).

Experimental procedure

Long and short crack data were obtained using a 60 kN servo-hydraulic testing machine operating at a frequency of 40 Hz, and the load ratio, R , was 0.5 in all tests. The crack length was measured using the direct current potential drop technique (23). Closure measurements were carried out using a back face strain gauge system incorporating an offset elastic displacement circuit (24).

Long crack data were obtained using single edge notched bend specimens with a width of 25 mm, thickness of 15 mm, and notch depth of 5 mm, tested in

Table 1 Composition of materials

Steel type	C	Mn	Si	Ni	Cr	Mo
Low strength steel	0.15	0.57	0.15	0.03	<0.02	<0.02
High strength steel	<0.2	—	—	2.5	1.5	0.5

four point bend loading. The loads were reduced in 5 per cent decrements and the crack was allowed to grow a distance of at least four times the size of the reversed plastic zone at each load range. The load-shedding procedure was continued until no further crack growth could be detected in 10^6 cycles and then the loads were incremented in 5 per cent steps.

The short through-thickness cracks were initiated at central slots in testpieces with a width of 25 mm and thickness of 15 mm. The pre-crack was grown using a load-shedding sequence with 10 per cent decrements to achieve near-threshold growth at a pre-crack length of approximately 5 mm. Then 2.5 mm was removed from the side faces of the testpiece by machining, and approximately 5 mm removed from the top, to leave a straight-fronted short through-thickness pre-crack of between 0.1 and 1.0 mm in length in a testpiece with a width of 20 mm and thickness of 10 mm. The specimens were stress-relieved at 650°C for one hour in a vacuum furnace prior to testing.

The short pre-cracks were subjected to fatigue loading in four point bend

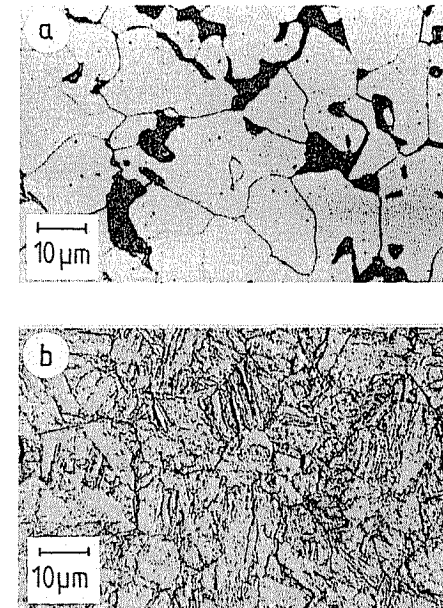


Fig 2 Microstructures: (a) low strength steel, (b) high strength steel Q1N

loading at initial ΔK values in the range $2\text{--}12 \text{ MNm}^{-3/2}$. If no crack growth was detected in 10^6 cycles the loads were increased by 5 per cent until crack growth occurred.

Results

The long crack data are shown in Fig. 3. When the applied ΔK was greater than approximately $7 \text{ MNm}^{-3/2}$, the opening stress intensity, K_{op} , measured by the back face strain gauge on reloading, was lower than the minimum stress intensity during the fatigue cycle, K_{min} , so that there was no effect of closure on the measured growth rate. When the applied ΔK was less than $7 \text{ MNm}^{-3/2}$, K_{op}

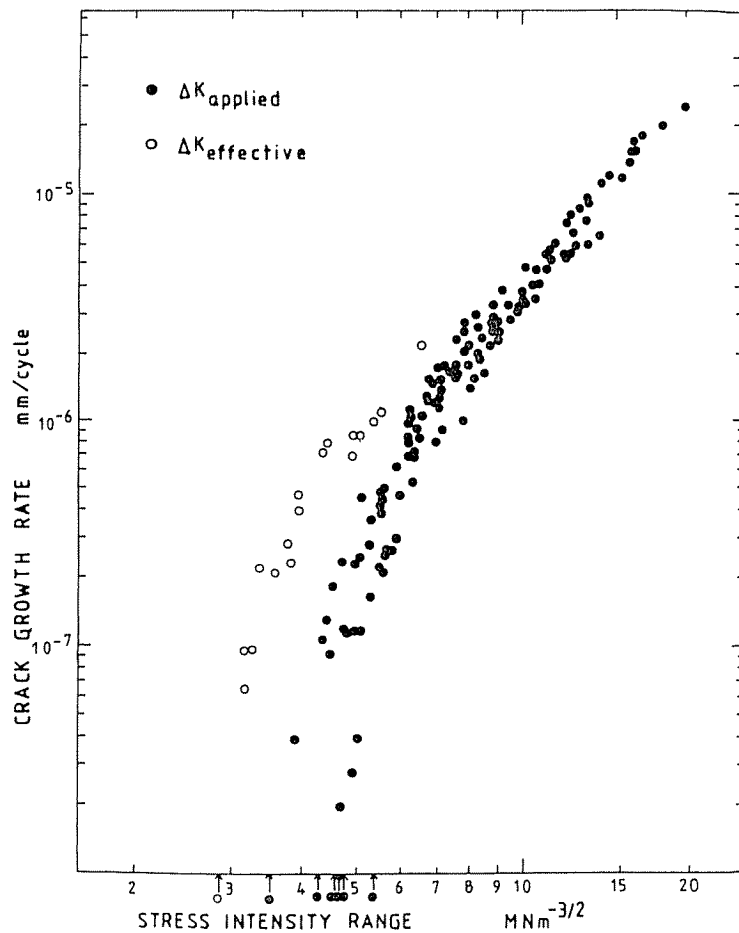


Fig 3 Long crack results in the near-threshold region for low strength steel. $R = 0.5$

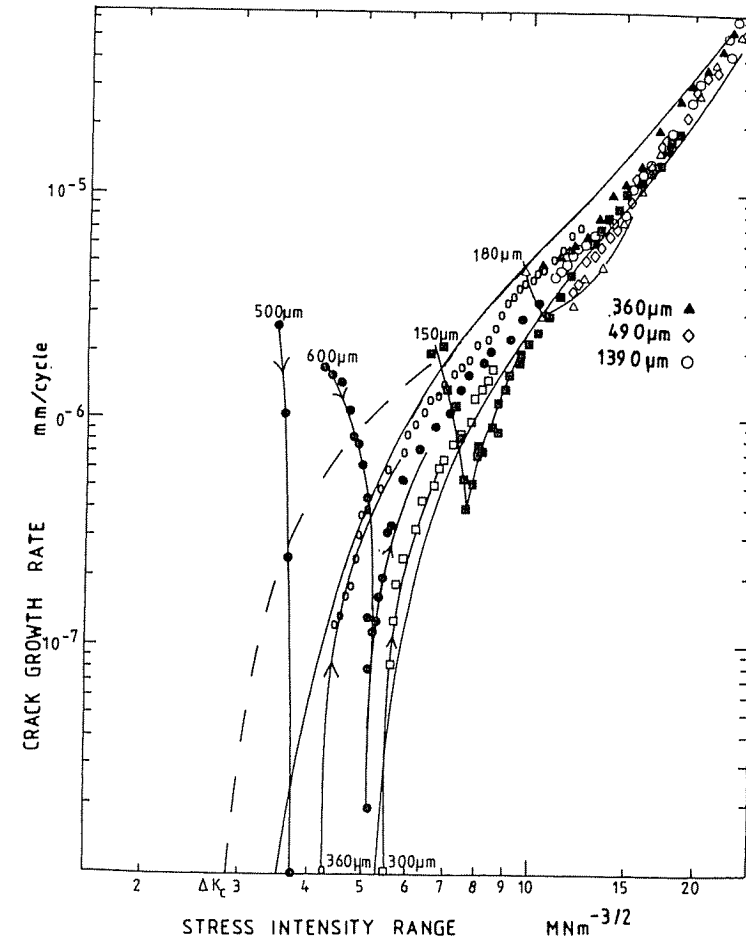


Fig 4 Short crack results compared with long crack results for low strength steel. Dashed line shows ΔK_{eff} data for long cracks. The initial lengths of short cracks are given in microns

was greater than K_{min} and the measured growth rate was reduced by the effect of closure. The threshold at $R = 0.5$ was equal to approximately $4.5 \text{ MNm}^{-3/2}$. The effective stress intensity range at which crack growth could not be detected, as determined by closure measurements, was approximately $3.0 \text{ MNm}^{-3/2}$.

The short crack data are compared with the long crack data in Fig. 4. Considering first the short cracks tested at lower initial ΔK values, it can be seen that some cracks grew at applied ΔK values below the measured long crack ΔK_{th} of $4.5 \text{ MNm}^{-3/2}$, sometimes at an initially decreasing growth rate. Other short cracks simply followed the long crack curve after commencing growth at ΔK values close to the long crack ΔK_{th} .

In order to apply the required stress intensity range to the short cracks that were tested at initial ΔK values greater than $7 \text{ MNm}^{-3/2}$, it was necessary to apply such high loads that the specimen was yielded over the whole width, although the change in applied moment-arm as a result of specimen deformation was negligible. Nonetheless, the growth rates for the short cracks (0.1–1.0 mm long) coincided with the long crack data. That is, within the sensitivity of the apparatus (which could detect $30 \mu\text{m}$ of crack growth), no short crack growth was observed for cracks of these sizes when the value of the initial applied ΔK was in the range in which long cracks were not affected by closure at a load ratio of 0.5.

Experimental work on a high strength steel

The material studied in a second set of experiments was a weldable alloy steel, Q1N, with a yield strength of 653 MNm^{-2} and an ultimate tensile strength of 743 MNm^{-2} . The composition is shown in Table 1. The material was water quenched and tempered at 640°C to give a tempered martensitic microstructure, as shown in Fig. 2(b).

Experimental procedure

Threshold ΔK_{th} values were measured for long cracks and for short cracks of both through-thickness and thumbnail geometries. The experimental procedures have been described previously (15)(24). Briefly, the long crack data were obtained using single edge notched bend specimens tested in four point bend loading and the short through-thickness crack data were obtained by growing a long pre-crack and removing the top of the specimen by machining. The short surface cracks were initiated at inclusions on unnotched testpieces, under loading conditions in which the surface of the testpiece was yielded. A stress-relief heat treatment was carried out before testing at load ratios between 0.2 and 0.7. Closure measurements were made during the long crack tests.

Results

The measured ΔK_{th} values are shown in Fig. 5 (15), plotted against the crack length on a logarithmic scale. It was found that the short through-thickness cracks of length 0.27–1.0 mm had ΔK_{th} values lower than the measured long crack ΔK_{th} of $4.8 \text{ MNm}^{-3/2}$, but higher than the value of the effective stress intensity range at threshold (ΔK_c) of approximately $3.0 \text{ MNm}^{-3/2}$. Therefore, the short through-thickness crack data fell in the region of ΔK in which long cracks were affected by closure.

However, for the short surface cracks of 0.1–0.4 mm in length, ΔK_{th} values close to the measured long crack ΔK_{th} of $4.8 \text{ MNm}^{-3/2}$ were obtained. This indicates that there is a variation in the ΔK_{th} values measured for short cracks of different geometries prepared by different techniques.

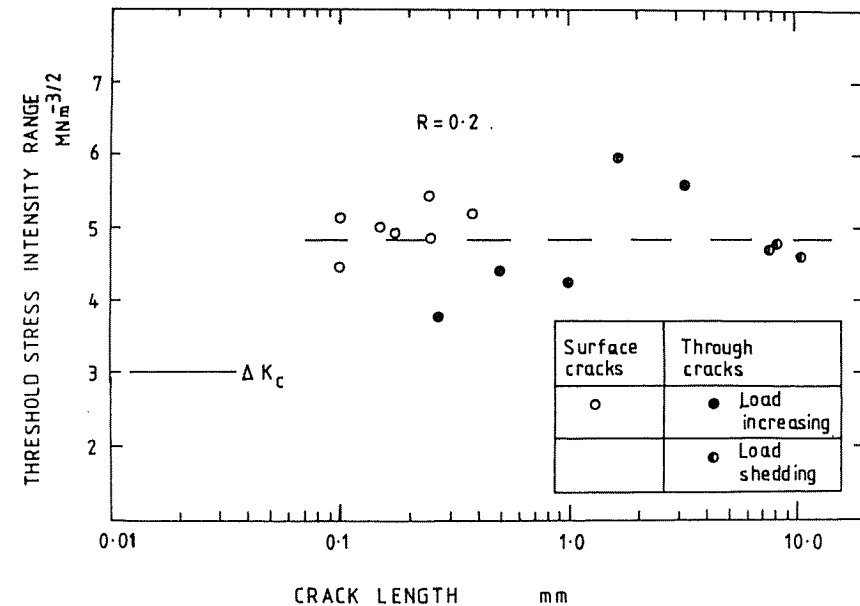


Fig 5 Threshold values of surface thumbnail and through-thickness cracks for high strength steel. Dashed line shows measured long crack threshold

Discussion

Discussion of results

Plasticity-induced closure arising from forces within the plastic wake is one of the most significant factors affecting the growth of fatigue cracks at low ΔK values. The concept has been used to explain the effect of load ratio on long crack ΔK_{th} values determined by conventional load-shedding threshold tests (25). If K_{op} is greater than K_{min} during the fatigue cycle, the effective stress intensity, ΔK_{eff} , will be lower than the applied ΔK , producing an elevation in the measured value of ΔK_{th} . It has been suggested that during a long crack threshold test the increase in closure as ΔK_{th} is approached is primarily a load-shedding effect (15). At high load ratios, however, and at higher applied ΔK values, there is minimal effect of plasticity-induced closure.

Experiments have been carried out in which part of the plastic wake behind the tip of a long crack is removed by electro-discharge machining (EDM) (15)(26). This process is shown in Fig. 6 for a long crack growing in the near-threshold region. The crack growth rate was approximately 6×10^{-8} mm/cycle for a crack that was 2.43 mm in length after a load-shedding sequence. Part of the wake was removed by EDM to leave 0.5 mm of wake behind the crack tip. The subsequent growth rate, at almost the same applied

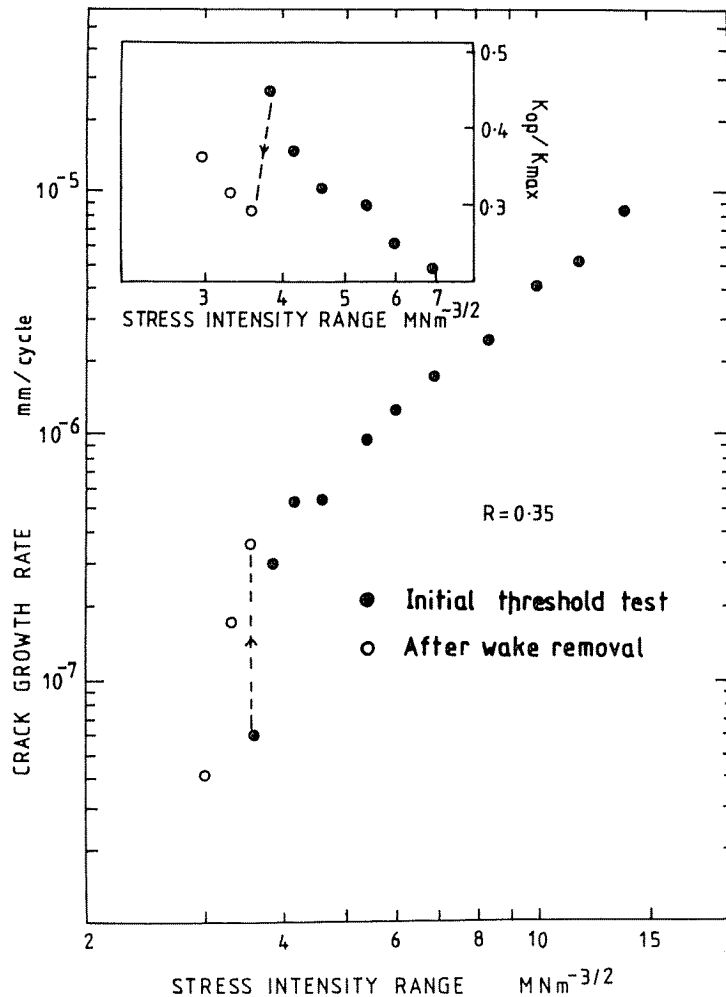


Fig 6 Growth rate and closure data showing the effect of wake removal (15)

ΔK , was found to have increased to approximately 4×10^{-7} mm/cycle, associated with a reduction in K_{op}/K_{max} from 0.45 to 0.29. This demonstrates that, in these experiments, significant effects of plasticity-induced closure were produced by parts of the plastic wake located more than 0.5 mm behind the crack tip. It has been calculated that the distance over which there is contact between the opposing fatigue faces may be up to 1–2 mm during a long crack threshold test (15).

The short through-thickness cracks were prepared by growing long cracks

under a load-shedding sequence into the threshold region and then machining away the material behind the crack tip. As for the EDM experiments described above, this method of preparation removed a large part of the plastic wake and it is deduced that the difference in behaviour between long and short cracks, shown in Fig. 4, arises simply from the fact that less plasticity-induced closure is associated with the short crack growth. At higher stress intensities, plasticity-induced closure becomes less significant and the results for long and short cracks lie on a single curve.

The experimental values of ΔK_{th} for short surface cracks in Q1N steel, however, were found to fall within the scatter-band of long crack values. The surface cracks were initiated at inclusions and grown to lengths in the range 0.1–0.4 mm under conditions of gross surface yielding ($R > 0.2$). Unloading then induces a compressive residual stress and if the stress-relief treatment of one hour at 650°C does not completely remove this stress, clamping forces could produce a closure effect during the subsequent determination of ΔK_{th} , such that the measured values were similar to those for long cracks, where plasticity-induced closure was operative. Support for this is given by crack closure measurements made on small thumbnail cracks grown in a region of surface plasticity. These gave K_{op}/K_{max} values identical to those determined for long cracks growing under elastic conditions at a low load ratio (22)(27).

The difference in behaviour observed for the two kinds of short cracks examined in the present work is therefore rationalized in terms of the effects of different residual stress fields on threshold behaviour.

The 'Kitagawa plot'

The 'anomalous behaviour' of physically short cracks is illustrated by region II of Fig. 1, in the graph of $\log \Delta \sigma_o$ against $\log a$. Here, experimental values of $\Delta \sigma_o$ are lower than would be predicted by either the LFM calculations based on ΔK_{th} (which works well for region III) or the endurance limit, for 10^7 or 10^8 cycles as appropriate (region I).

One reason for the anomalous behaviour is that the plasticity associated with crack growth increases rapidly with applied stress level, so that the LFM analysis becomes increasingly inaccurate. Miller (28) has shown that deviation from region III behaviour first occurs at a crack length such that the applied stress level exceeds one third of the cyclic yield stress. For monotonic loading, the maximum extent of the plastic zone in plane strain, R_{IY} , is given by (29)

$$R_{IY} = 0.16(K/\sigma_y)^2 = 0.16(\sigma_{app}^2/\sigma_y^2)\pi a \quad (4)$$

where σ_{app} is the applied stress. For $\sigma_{app} = \sigma_y/3$, the ratio of plastic zone size to crack length, $R_{IY}/a = 0.056$. The size of the reversed plastic zone is often obtained by substituting $2\sigma_y$ for σ_y in equation (4), so that the ratio of reversed plastic zone to crack length is approximately 0.014. The size of plastic zone increases initially with σ_{app}^2 , but then more rapidly as σ_{app} approaches σ_y .

The results given in Figs 3 and 4 show that for values of $\Delta K > 7 \text{ MNm}^{-3/2}$ the calculated values of da/dN for initially quite short cracks in structural steel of modest yield strength are identical to those measured on specimens containing long cracks, even though the short crack testpieces have undergone substantial general plastic yielding. It is remarkable that the results agree so well, for a value of ΔK calculated as if the loading were elastic. It is possible that, after the first few cycles, the general plasticity in the specimen as a whole 'shakes down' through cyclic hardening processes, eventually approaching saturation, so that the overall specimen response progressively becomes quasi-elastic, with the elastically calculated ΔK characterizing behaviour in the crack tip region.

If cyclic hardening can rapidly lead to a quasi-elastic response in specimens which have undergone gross yielding, it seems unlikely that the main cause of anomalous short crack behaviour is the increase of plastic zone size with applied stress level. An alternative possibility is that the different amounts of closure associated with short cracks produce relationships between the applied and effective stress intensity ranges which are different from those for long cracks. As described earlier in the paper, different types of residual stress distribution are associated with different sources of short cracks, so that details of behaviour must be assessed on an individual basis. Presumably, however, a lower bound is given by the complete absence of closure, e.g., for solidification cracks, or cracks for which stress-relief annealing has been completely effective.

The essential point is whether or not the line based on ΔK_{th} in Fig. 1 represents the 'no-closure' situation, because it is clear that the distribution of plasticity in the plastic wake can strongly affect the value of ΔK_{th} in a load-shedding test, unless the stress ratio, R , is high. The results of Kitagawa and Takahashi (Fig. 1) give a ΔK_{th} value of $15.5 \text{ Kgmm}^{-3/2}$ ($4.8 \text{ MNm}^{-3/2}$) for $R = 0.04$. This is compatible with their results, recognizing that the cracks of interest were semi-circular and much smaller than testpiece dimensions. The appropriate value of Q in equation (2) is 0.66 so that the relationship between ΔK and $\Delta\sigma_o$ becomes

$$\Delta K = 0.66 \Delta\sigma_o (\pi a)^{1/2} \quad (5)$$

The value of $\Delta K_{th} = 4.8 \text{ MNm}^{-3/2}$ for $R = 0.04$ is comparable with (although perhaps a little lower than might be expected from) a value of $\Delta K_{th} = 4.8 \text{ MNm}^{-3/2}$ for $R = 0.2$ obtained by James and Knott for a quenched and tempered steel of similar yield strength (15). In the latter case, measurements of closure indicated that plastic wake closure was highly significant in the $R = 0.2$ results and that the 'closure-free' value of ΔK_{th} , i.e., ΔK_c , was approximately $3.0 \text{ MNm}^{-3/2}$. A similar value applies to the lower strength structural steel, for which the experimental data are given in Fig. 3.

Recalculation of the long crack data in Fig. 1 using $\Delta K_c = 3.0 \text{ MNm}^{-3/2}$ reduces all the values of $\Delta\sigma_o$ by a factor of $(3/4.8)$, i.e., the position of the line in the log : log plot is lowered by a constant amount (see equations (1) and (2)

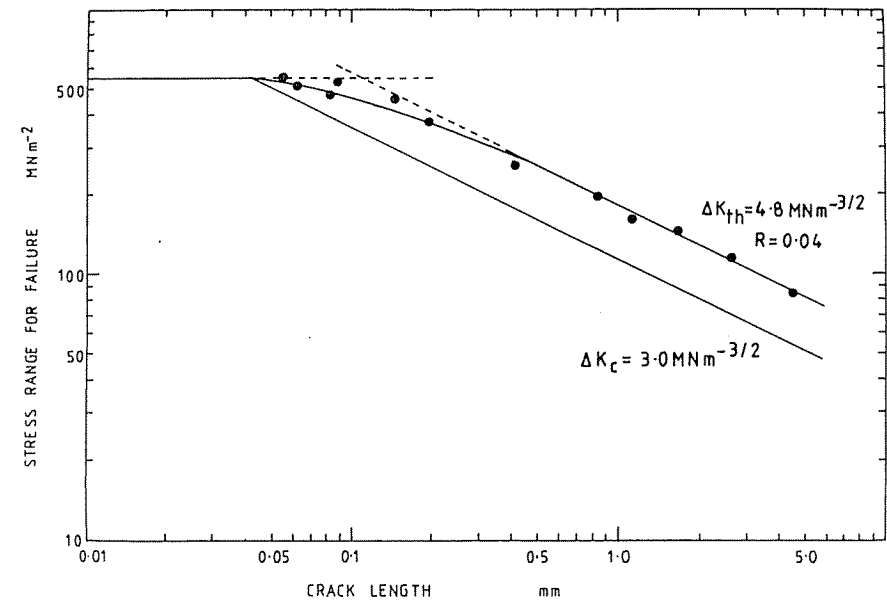


Fig 7 Effect on 'Kitagawa plot' (8) of recalculating long crack line using a closure-free threshold, ΔK_c

and Fig. 7). The effect of this shift is such as to provide an effective lower bound to all the data points. The inference is then that most of the 'anomalous' short crack behaviour observed here is attributed to an artefact of the long crack threshold test, i.e., the effect of closure at low stress ratio.

In terms of engineering design, it would seem that a rather good lower bound is obtained from the endurance limit and the value of stress calculated from the 'effective' threshold, $\Delta K_c = 3.0 \text{ MNm}^{-3/2}$. If a modest safety factor is applied to these bounds, integrity should be assured for the stressing situations envisaged, provided that gross variations from the accepted material properties (defect populations) do not occur. This can be achieved either by attention to quality control in fabrication and NDT or by consistency of materials processing.

The above discussion refers to cracks grown in air. It has been found that ΔK_c for cracks in vacuum is higher than that in air (31) and the position of the lower bound line in Fig. 7 would be altered accordingly. Tests in vacuum simulate the growth of cracks from buried defects.

An example of the use of ΔK_c in 'lifing'

The detailed assessment of the fatigue life of a welded component which is part of a vehicle demands a knowledge of the loading spectrum to which it is

subjected during service. In general, this is likely to comprise a large number of low amplitude cycles, each produced by a revolution of the vehicle's wheels on smooth roads or rail-tracks, together with a smaller number of higher amplitudes, associated with rough surfaces, such as pot-holes in roads or joints and welds on rail-tracks. Additionally, a few very high amplitudes may be experienced, due to loading by passengers or freight, or to the occasional onset of resonance. The lifing procedures involved may be appreciated by an illustrative example, using simplified figures taken from a paper by McLester, which shows the loading spectra for locomotive and freight bogies (30).

In approximately 200 miles of travel, the number of wheel revolutions is of the order of 10^5 . McLester's figures show that the spectra contain many cycles at stress levels below 50 MNm^{-2} and rather few at higher levels. For simplicity, we take 20 cycles at 100 MNm^{-2} and 10^3 cycles at 65 MNm^{-2} . The assumptions made are that NDT is capable of detecting an edge crack of 1 mm in size and that a proposal has been made that a safe inspection period is every 10^8 cycles (approximately 2×10^5 miles or 1–2 years). A traditional LFM analysis would wish to ignore all cycles at stresses such that the values of ΔK were below the threshold ΔK_{th} , but this philosophy would be open to question in the light of 'anomalous' short crack growth behaviour, which tends to indicate that cracks of less than 1 mm in length (the NDT limit) could grow at ΔK values less than ΔK_{th} .

If, however, the short crack behaviour is 'anomalous' only because closure effects operate in long crack threshold tests, it would appear that a threshold philosophy could be maintained, provided that the 'closure-free' value of ΔK_{th} , ΔK_c , were employed. Our results suggest that ΔK_c is approximately $3.0 \text{ MNm}^{-3/2}$ for structural steel, which, for a 1 mm edge crack, corresponds to an applied stress of approximately 50 MNm^{-2} . We conclude, therefore, that in 10^5 total cycles for the simplified loading spectrum, the only cycles of importance are the 20 at 100 MNm^{-2} and the 10^3 at 65 MNm^{-2} . During the proposed inspection period of 10^8 cycles, the component is therefore subjected to 2×10^4 cycles at 100 MNm^{-2} and 10^6 cycles at 65 MNm^{-2} . Using the expression

$$da/dN = 10^{-11} \Delta K^3 \quad (6)$$

where $\Delta K = 1.12 - \Delta\sigma(\pi a)^{1/2}$ for an edge crack, it may be calculated using a simple Miner's Law summation, that a crack, initially just below 1 mm in length (i.e., just undetectable by NDT) grows to approximately 2.5 mm in 10^8 cycles (ignoring the fact that ΔK_c will be exceeded by stresses in the range 50 – 30 MNm^{-2} as the crack length increases from 1 to 2.5 mm). Final crack lengths of this order are unlikely to cause failure by plastic collapse or fast fracture in tough, structural steels, and so the proposed inspection period is deemed to be appropriate. Any crack found during inspection would be repaired.

The above calculation is illustrative, rather than precise, but does demonstrate the lifing principles involved. Specifically, we suggest that, if the 'closure-free' value, ΔK_c , is employed, a threshold philosophy may be maintained, uncomplicated by any 'anomalous' short crack behaviour.

Conclusions

In considering the behaviour of physically short cracks it is essential to take into account the residual stress fields surrounding the cracks. In long crack threshold tests at low load ratios, plasticity-induced closure in the wake of the growing crack influences crack growth rates. The results of this study indicate that different amounts of closure in short crack specimens may account for much of the 'anomalous' behaviour of physically short cracks. Predictions of fatigue life using a closure-free value of the threshold may therefore be satisfactory in applications in which reliance is placed on NDT control.

Acknowledgements

The authors wish to thank Professor R. W. K. Honeycombe, FRS, and Professor D. Hull for the provision of research facilities. They are grateful to the SERC and British Rail Research Laboratories, Derby (JMK) and the Ministry of Defence, Procurement Executive (MNJ) for financial support.

References

- (1) TAYLOR, D. and KNOTT, J. F. (1982) Growth of fatigue cracks from casting defects in nickel-aluminium bronze, *Metall. Technol.*, **9**, 221–228.
- (2) PEARSON, S. (1975) Initiation of fatigue cracks in commercial Aluminium alloys and the subsequent propagation of very short cracks, *Engng Fracture Mech.*, **7**, 235–247.
- (3) TANAKA, K., NAKAI, Y., and YAMASHITA, M. (1981) Fatigue growth threshold of small cracks, *Int. J. Fracture*, **17**, 519–533.
- (4) LANKFORD, J. (1982) The growth of small fatigue cracks in 7075-T6 aluminium, *Fatigue Engng Mater. Structures*, **5**, 233–248.
- (5) DE LOS RIOS, E. R., TANG, Z., and MILLER, K. J. (1984) Short crack fatigue behaviour in a medium carbon steel, *Fatigue Engng Mater. Structures*, **7**, 97–108.
- (6) BROWN, C. W., KING, J. E., and HICKS, M. A. (1984) Effects of microstructure on long and short crack growth in nickel base superalloys, *Metal Sci.*, **18**, 374–380.
- (7) SURESH, S. and RITCHIE, R. O. (1984) The propagation of short fatigue cracks, *Int. Met. Rev.*, **29**, 445–476.
- (8) KITAGAWA, H. and TAKAHASHI, S. (1976) Applicability of fracture mechanics to very small cracks or cracks in the early stage, *Proceedings of the 2nd International Conference on the Behaviour of Materials*, Boston, pp. 627–631.
- (9) TSUBOTA, M., KING, J. E., and KNOTT, J. F. (1984) Crack propagation and threshold behaviour in Ni-base superalloys and its implications for component life assessment, *First Parsons International Turbine Conference*, Dublin (Institution of Mechanical Engineers, London), pp. 189–195.
- (10) COLES, A. (1979) Material Considerations for Gas Turbines, *Proceedings of the Third International Conference on Mechanical Behaviour of Materials*, Cambridge, Vol. 1, pp. 3–11.
- (11) THOMPSON, A. W. and BERNSTEIN, I. M. (1977) Selection of structural materials for hydrogen pipelines and storage vessels, *Int. J. Hydrogen Energy*, **2**, 163–173.
- (12) TETELMAN, A. S. and ROBERTSON, W. D. (1963) Direct observation and analysis of crack propagation in iron-3% silicon single crystals, *Acta Met.*, **11**, 415–426.
- (13) BROOKSBANK, D. and ANDREWS, K. W. (1972) Stress fields around inclusions and their relation to mechanical properties, *J. Iron Steel Inst.*, **210**, 246–255.
- (14) CLARK, G. and KNOTT, J. F. (1977) Effects of notches and surface hardening on the early growth of fatigue cracks, *Met. Sci.*, **11**, 345–350.
- (15) JAMES, M. N. and KNOTT, J. F. (1985) An assessment of crack closure and the extent of the short crack regime in Q1N (HY80) steel, *Fatigue Engng Mater. Structures*, **8**, 177–191.

- (16) CHAUHAN, P. and ROBERTS, B. W. (1979) Fatigue crack growth behaviour of short cracks in a steam turbine rotor steel—an investigation. *Metall. Mater. Technol.*, **11**, 131–136.
- (17) USAMI, S. and SHIDA, S. (1979) Elastic–plastic analysis of the fatigue limit for a material with small flaws, *Fatigue Engng Mater. Structures*, **1**, 471–481.
- (18) ROMANIV, O. N., SIMINKOVICH, V. N., and TKACH, A. N. (1981) Near-threshold short fatigue crack growth, *Proceedings of the 1st International Conference on Fatigue Thresholds*, Stockholm, Vol. 2, pp. 799–807.
- (19) McCARVER, J. F. and RITCHIE R. O. (1982) Fatigue crack propagation thresholds for long and short cracks in Rene 95 nickel-base superalloy, *Mater. Sci. Engng*, **55**, 63–67.
- (20) KING, J. E. and KNOTT, J. F. (1980) The effects of crack length and shape on the fracture toughness of a high strength steel 300M, *J. Mech. Phys Solids*, **28**, 191–200.
- (21) BYRNE, J. and DUGGAN, T. V. (1981) Influence of crack geometry and closure on the fatigue threshold condition, *Proceedings of the 1st International Conference on Fatigue Thresholds*, Stockholm, Vol. 2, pp. 759–775.
- (22) JAMES, M. N. and SMITH, G. C. (1984) Short crack behaviour in A533B and En8 steels, *Proceedings of 6th International Conference on Fracture (ICF6)*, New Delhi, Vol. 3, pp. 2117–2124.
- (23) RITCHIE, R. O., GARRETT, G. G., and KNOTT, J. F. (1971) Crack-growth monitoring: optimisation of the electrical potential technique using an analogue method, *Int. J. Fracture Mech.*, **7**, 462–467.
- (24) JAMES, M. N. and KNOTT, J. F. (1985) Critical aspects of the characterization of crack tip closure by compliance techniques, *Mater. Sci. Engng*, **72**, L1–L4.
- (25) NAKAI, Y., TANAKA, K., and NAKANISHI, T. (1981) The effects of stress ratio and grain size on near-threshold fatigue crack propagation in low-carbon steel, *Engng Fracture Mech.*, **15**, 291–302.
- (26) MINAKAWA, K., NEWMAN, J. C., and McEVILY, A. J. (1983) A critical study of the crack closure effect on near-threshold fatigue crack growth, *Fatigue Engng Mater. Structures*, **6**, 359–365.
- (27) JAMES, M. N. and SMITH, G. C. (1983) Surface microcrack closure in fatigue: a comparison of compliance and crack sectioning data, *Int. J. Fracture*, **22**, R69–R75.
- (28) MILLER, K. J. (1984) Initiation and growth rates of short fatigue cracks, *Eshelby Memorial Symposium*, Sheffield, pp. 477–500.
- (29) RICE, J. R. and TRACEY, D. M. (1973) *Numerical and computational methods in structural mechanics* (Edited by Fenves, S. J. et al.), (Academic Press, New York).
- (30) McLESTER, R. (1977) Fatigue problems in land transport, *Met. Sci.*, **11**, 303–307.
- (31) JAMES, M. N. and KNOTT, J. F. (1985) Near-threshold fatigue crack closure and growth in air and vacuum, *Scripta Met.*, **19**, 189–194.